

PHYSICAL REVIEW D

PARTICLES, FIELDS, GRAVITATION, AND COSMOLOGY

THIRD SERIES, VOLUME 48, NUMBER 10

15 NOVEMBER 1993

Performance of the South Pole Air Shower Experiment during 1987 to 1992

J. Beaman, A. M. Hillas, P. A. Johnson, J. Lloyd-Evans, N. J. T. Smith, and A. A. Watson
Physics Department, University of Leeds, Leeds LS2 9JT, United Kingdom

J. van Stekelenborg, T. K. Gaisser, J. C. Perrett, J. P. Petrakis, and T. S. Stanev
Bartol Research Institute, University of Delaware, Newark, Delaware 19716
(Received 18 June 1993)

We describe the performance of an extensive air shower array sited at the geographic South Pole from its construction in 1987 to the austral summer of 1991. The stability of the array over this four year period when the detectors were subjected to temperature cycling over a 60°C range is evaluated. The analysis techniques used to determine the core position and direction of the shower are discussed, along with checks on the angular resolution and pointing accuracy of the array, found to be 0.9° and $0.2^\circ \pm 0.5^\circ$ respectively.

PACS number(s): 95.55.Ka, 95.55.Vj, 95.85.Pw

I. INTRODUCTION

The South Pole Air Shower Experiment (SPASE) is a joint collaboration between scientists in the Physics Department at the University of Leeds and the Bartol Research Institute at the University of Delaware. The experiment is an extensive air shower array designed to study cosmic rays above 10^{14} eV, specifically to monitor ultrahigh energy γ rays which travel undeviated in the galactic magnetic field from potential point sources such as x-ray binaries. The initial construction of the array is discussed in Smith *et al.* [1]. In this configuration the array consisted of 16×1 m² scintillation detectors placed on a 30 m triangular grid pattern 200 m from the geographic South Pole. The pertinent details of the array are given in Table I. The array was sited at the South Pole following a suggestion by Hillas [2] to take advantage of the high altitude of the site, the circumpolar nature, and hence constant viewing of the candidate sources, the constant zenith angle of these sources, and the high number of potential sources visible in the southern hemisphere. In this paper we describe the performance and stability of the telescope since it was constructed and the analysis techniques used to determine the arrival direction of the showers. The techniques used to search for point sources of emission and the result of such searches are described in an accompanying paper [3].

II. THE DATA SAMPLE

The first extensive air shower was observed by the experiment on 21 December 1987. From then until the end of 1992 the array has performed with an on time

approaching 90% during the winter (February to October) and an on time of 40% during the summers when array calibrations and modifications are performed. The maximum temperature experienced by the detectors was -16°C , the minimum -74°C .

The data are split into three epochs during the analysis. The first epoch consists of data recorded with the original array configuration. During the second epoch, from January to November 1989, a recurrent problem with the absolute time recorded with each event means that a substantial fraction of this data set is unreliable for source searching and has been omitted from the analysis. The last epoch includes an additional eight ("guard ring") detectors which were added in December of 1989 around the edge of the array at an average distance of 45 m. These eight detectors only record particle densities and are used to help determine whether the core falls inside or outside the main array of 16 modules. At the same time a layer of lead was added to the main array detectors to improve the angular resolution of the telescope by using the Rossi transition effect [4]. Excluding the 1989 data, a total usable data set of 58.8 million recorded events has been logged, during an exposure of 4.4×10^{15} cm² s. Of these recorded events 56.0 million events were selected for source searching using criteria discussed later. The three epochs are summarized in Ta-

TABLE I. Array details.

Latitude	90° S
Altitude	2835 m (695 g cm ⁻²)
Enclosed area	6235 m ²
Energy threshold	50 TeV

TABLE II. Data epochs.

Epoch	Date	No. of events		No. of dets	Lead
		Recorded	Selected		
1	03/88–01/89	10.9×10^6	10.6×10^6	16	No
2	01/89–11/89	21.8×10^6	None used	16	No
3	01/90–11/91	47.9×10^6	45.4×10^6	24	Yes
Total		80.7×10^6	56.0×10^6		

ble II. The present configuration of the experiment is shown in Fig. 1.

III. ARRAY CALIBRATIONS

To determine the arrival direction of the primary cosmic ray it is necessary to know the coordinates of each detector in the array to centimetric accuracy and the orientation of the array with respect to the Greenwich meridian. The SPASE array has the unique complication that the plateau upon which it is constructed is known to move at a rate of ~ 10 m per year. However, any lateral shift in the array as a whole is unimportant and only relative shifts between detectors, or a change in orientation, need be accounted for. The coordinates and orientation of the SPASE detectors were surveyed in December 1987 and resurveyed in December 1988 and were found to be consistent within measurement errors. The coordinates were determined with professional surveying equipment and the orientation was determined using the alignment of the Sun and detectors during the week long dawn and dusk. The error in the coordinates was determined to be ± 2 cm and that in the telescope orientation to be $\pm 0.2^\circ$.

Another important calibration for an extensive air shower array is the relative delay between each detector, the time taken for each light pulse from each scintillation

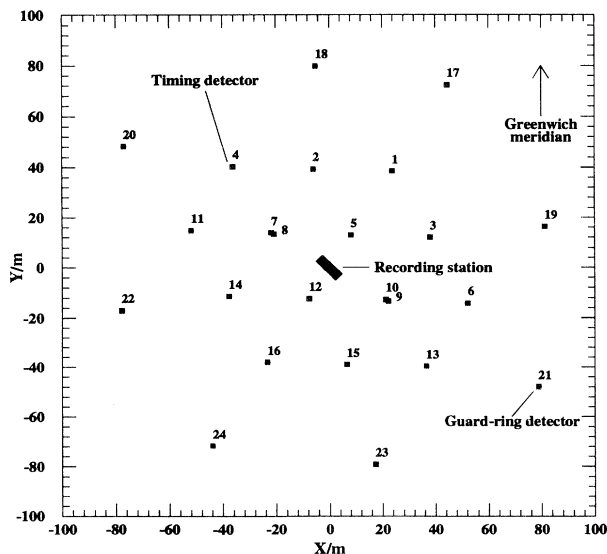


FIG. 1. Map showing the 1991 configuration of the SPASE array.

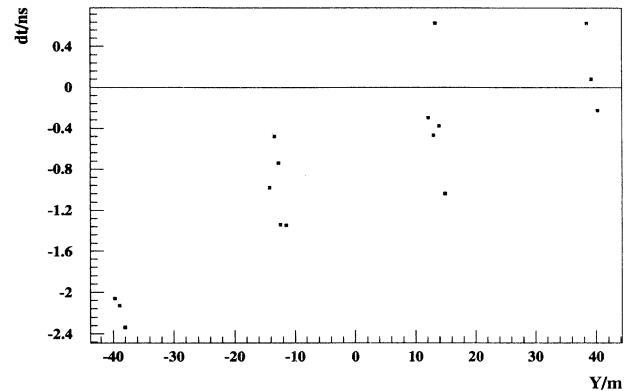


FIG. 2. The variation of the discrepancy in relative timing delays between detector channels as a function of the y Cartesian coordinate of the detector (“north-south”).

detector to be recorded and digitized. These delays are used when determining shower direction and need to be known to subnanosecond precision for an array as small as SPASE. Results presented at the Dublin Conference [5] indicated a strong harmonic in the azimuthal distribution of showers recorded and the possibility that this asymmetry was due to incorrect delays was discussed. These delays were subsequently remeasured during the 1991 to 1992 summer season and a systematic difference was observed across the array. Figure 2 shows the difference in measured delays plotted as a function of the north-south coordinate of the detector. Although the maximum discrepancy was 2.1 ns, the systematic nature of these discrepancies effectively caused the array to appear tilted in a north-south sense, causing the observed asymmetry. This north-south systematic error arises due to a conspiracy between the regular numbering system used for the detectors and an error in delay measurements across the time-to-digital converter (TDC) modules. A reanalysis using the new values of the delays shows a small second harmonic of 2.1% for the 1991 data set, Fig. 3(a), which is due to the geometry of the array, with the preferential triggering rate along the major axis. The phase of the second harmonic, calculated for the 1991 data, is $242^\circ \pm 1^\circ$. The size of the amplitude and the phase also depend on the triggering requirement. This has been verified by a rough Monte Carlo calculation: showers of typical size, age ($s=1.3$), and zenith angle ($\theta = 24.8^\circ$) are generated for a particular azimuth (e.g., 10°) on a 1 m^2 grid. Only air showers that have cores inside the main array of 16 detectors are selected, i.e., approximately 6250 showers for each azimuthal direction. The fraction of events that actually trigger the array is subsequently calculated and plotted for each azimuth, assuming a triggering requirement of 6 detectors as was the case in 1991 [Fig. 3(b)]. The Monte Carlo simulation results in an azimuthal distribution which shows a weak second harmonic with an amplitude of 1.6% and a phase of 241° , consistent with the actual SPASE data. In spite of the crude assumptions made in the Monte Carlo calculations, the simulated distribution mimics most of the main features of the actual data.

The stability of the delays can be derived from the data

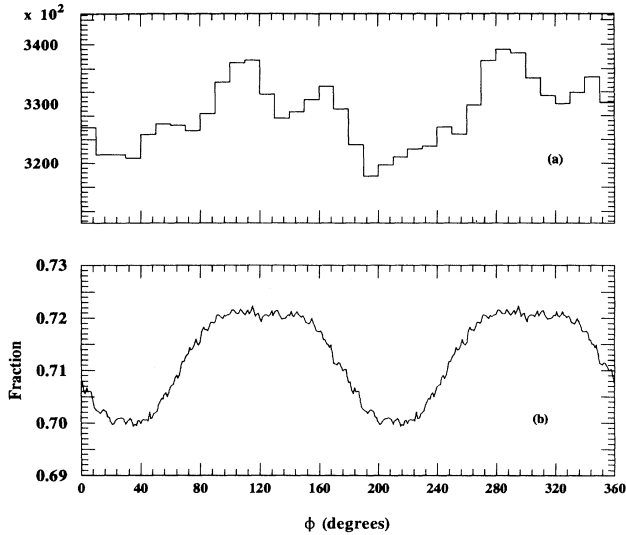


FIG. 3. (a) Azimuthal distribution of cosmic rays in 1991 as recorded by the SPASE telescope. Note that the zero point is highly suppressed. (b) Azimuthal distribution from Monte Carlo simulations. The simulated showers had an $s(30)$ of 2.0 m^{-2} and a zenith angle of 24.8° . The distribution results from a 6 detector triggering condition.

by studying the difference between the observed time for each detector and that predicted, assuming shower structure is correctly accounted for. The mean of these residuals should be zero and any change in a detector delay will be reflected by a change in the residuals. Examples of the time dependence of these residuals over the duration of the experiment are given in Fig. 4. The small offset from zero in these graphs is mainly due to a slight error in the shower structure discussed later and is less than 200 ps for all detectors. The graph for detector 4 shows a glitch which was identified as being due to a fault with a transistor in the discriminator circuitry. When identified changes to the system, such as a change in the operating voltage for a photomultiplier tube, are accounted for these residuals are found to have a rms

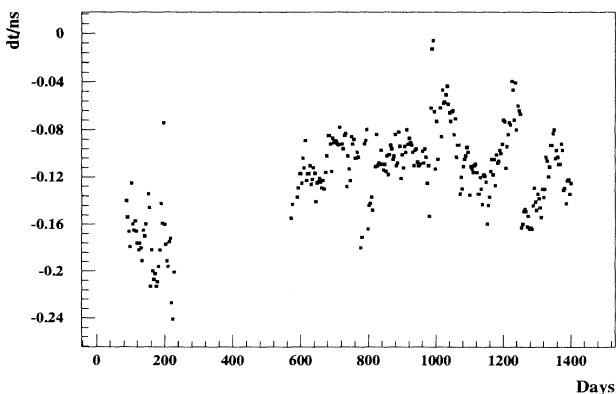


FIG. 4. The variation of the timing residual between observed and predicted arrival times at detectors over the duration of the experiment for a typical detector channel.

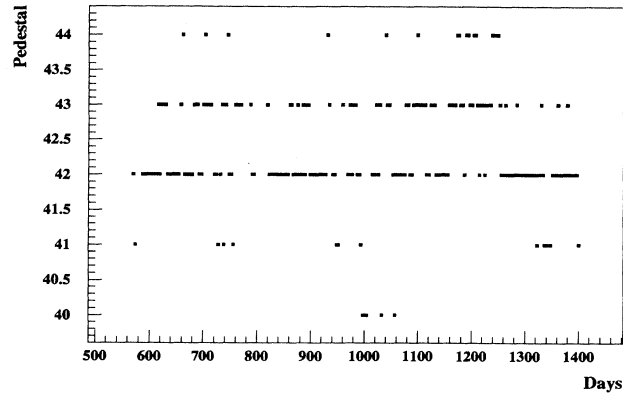


FIG. 5. The variation of the injected ADC charge pedestal over the duration of the experiment for typical detector channels. During the first year of operation the pedestals were automatically subtracted. Also, in 1990 and 1991 several runs were performed in coincidence with Čerenkov detectors during which the pedestals were subtracted. This accounts for the 0 values in the figure.

scatter of 50 ps. The stability of the delays is better than that so far attained in similar experiments in more temperate regions, presumably due to the lack of diurnal effects, use of buried cables which experience relatively small temperature fluctuations, and the few interventions from physicists during the winter months.

The other fundamental measurement made with each detector is the particle density in the extensive air shower front. LeCroy 4300 charge integrating analogue-to-digital converters (ADC's) are used with pedestals being of the order of 50 ADC counts. In the SPASE experiment one particle is defined as the mean signal from an ionizing particle passing vertically through the scintillator. As the conversion from ADC counts to particle density is ~ 16 counts per particle any major fluctuations in these pedestals, can severely affect the density measurement, especially at low particle densities. The stabilities of these pedestals over the duration of the experiment are shown in Fig. 5.

As discussed in Smith *et al.* [1] two discriminators are used in each detector channel. A low level discriminator, set to one-third of the signal detected from a vertically traversing particle, is used for prompt timing, and a second discriminator, set at the one particle level, is used to determine the array trigger criterion. The rate at which these detectors fire gives an indication of any fluctuation in noise or gain of the photomultiplier. The discriminator trigger rate is dependent upon the atmospheric pressure and temperature and must be corrected before any interpretation is made. The pressure effect for the one-particle discriminator level has been measured for the SPASE array to be $-0.54 \pm 0.05\% \text{ mb}^{-1}$. The temperature correction has not been quantified but, being a factor of 40 smaller than the pressure correction (Watson 1988, Internal Haverah Park Report), is relatively unimportant. The overall event rate gives a good indication of the stability of the telescope. The pressure correction coefficient for the overall rate is $-0.74 \pm 0.02\% \text{ mb}^{-1}$, as shown in Fig. 6.

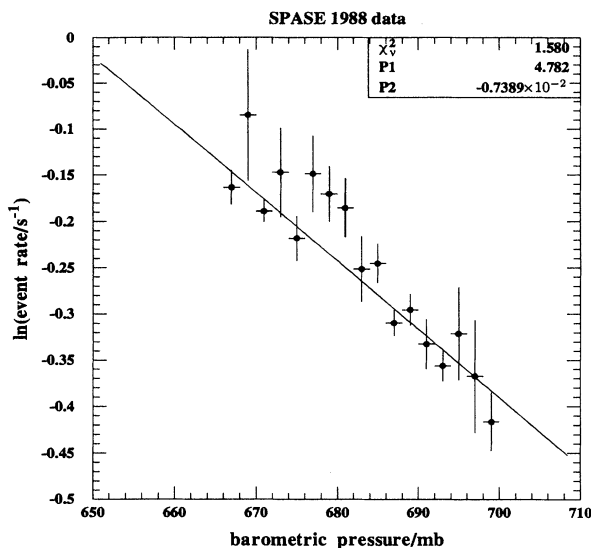


FIG. 6. Logarithm of the event rate versus barometric pressure during 1988.

The angular resolution and pointing accuracy of the SPASE array will be discussed in detail later in this paper.

IV. DATA ANALYSIS

The data recorded at the South Pole are analyzed at the home institutes using two independent analysis programs, one written in Fortran run on a Vax 4000 computer, the other written in Pascal running on a Sun SPARC workstation cluster. When the same selection criteria are applied to the data set and the same representation for the shower front is being used, the mean difference between the arrival direction of the primary cosmic ray determined by these two independent programs is $0.018 \pm 0.0005^\circ$, with a rms scatter of 0.02° . A

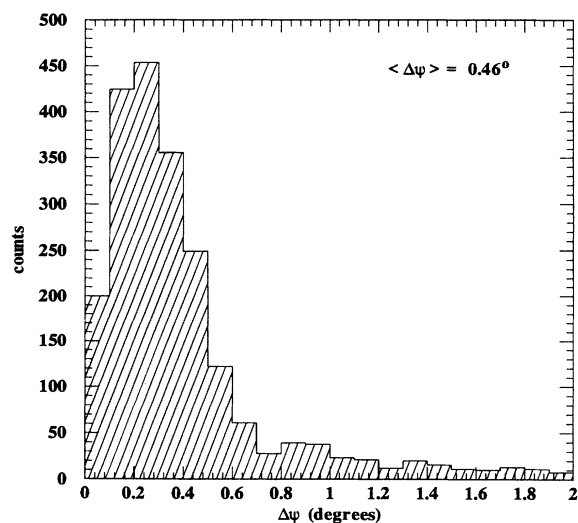


FIG. 7. Distribution of space angle difference between the Bartol and Leeds analysis schemes for the 1990 to 1991 data.

different approach to the minimization procedure in these programs accounts for this residual difference. However, the Leeds and Bartol groups use slightly different shower front parametrizations and selection criteria, which results in a mean difference between assigned arrival directions of $0.46 \pm 0.01^\circ$, with a rms scatter of 1.2° , see Fig. 7. More important, there is no systematic effect in the assigned values for zenith angle or azimuthal direction. The difference in assigned arrival directions is a factor of 2 smaller than the intrinsic angular resolution of the array. The different shower front parametrizations are each consistent with the data and the results are stated to give an indication of inherent uncertainties.

The direction of the primary cosmic ray is determined in both analyses by minimizing the quantity

$$\tau^2 = \sum_{\text{all dets}} \frac{[t(i)_{\text{obs}} - t(i)_{\text{expt}}]^2}{\sigma^2(i)},$$

where $t(i)_{\text{obs}}$ and $t(i)_{\text{expt}}$ are the observed and predicted times at each detector and $\sigma(i)$ is the associated uncertainty in the expected time. As these uncertainties are derived from a non-Gaussian distribution, the quantity τ^2 will not behave directly as chi squared, although it is assumed that the operational behavior is the same, i.e., the minimum of τ^2 gives the “best-fit” direction.

To determine the predicted time that the shower front strikes each detector it is necessary to have some representation of the shower front and the uncertainty associated with each recorded time. In the SPASE analysis these parameters, the shower front curvature and timing weights, are determined as a function of the particle density at a detector and the distance of that detector from the shower axis. These parameters were also determined from Monte Carlo simulations of the development of an extensive air shower and then compared to measurable parameters in the data set.

Figure 8 shows the timing residual ($t_{\text{obs}} - t_{\text{expt}}$) as a

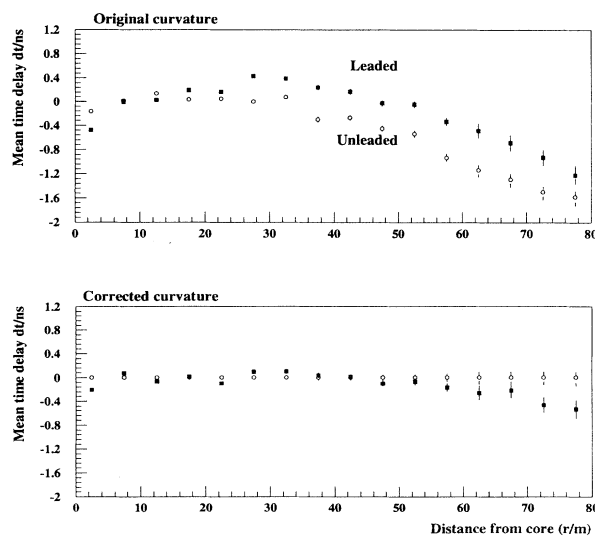


FIG. 8. The timing residual as a function of distance from the shower axis averaged over all detectors and all recorded particle densities.

function of axial distance, averaged over all detectors and particle densities. If the shower front curvature and timing weights are correctly accounted for, then the points in this figure should lie on the line $y = 0$. It can be seen that the maximum error associated with these representations is 1.2 ns at 80 m, corresponding to a maximum error in arrival direction of 0.25° , small in comparison to the angular resolution of the array, discussed later. Using this graph the shower front representation may be slightly modified to account for the small error involved. Figure 8 also shows the timing residuals for the modified representation.

The fluctuations in the arrival times are determined by measuring the spread of the expected minus the recorded time at a particular detector. Figure 9 shows the width of the timing residuals as a function of axial distance, again averaged over all detectors and recorded particle densities.

The parametrization of curvature and timing weights for the unleaded data from 1988 to 1989 is given by

$$dt(r, S) = -6.426 + 0.0461r + (6.34 + 0.001765r^2)/\sqrt{S}, \quad (1)$$

$$\sigma^2(r, S < 6.5) = 0.6 + 42.25(0.46 + 0.00521r + 0.000302r^2)^2/S^2, \quad (2)$$

$$\sigma^2(r, S \geq 6.5) = 0.6 + 6.5(0.46 + 0.00521r + 0.000302r^2)^2/S. \quad (3)$$

Two sets of curvature corrections and timing weights have been derived for the "leaded" data at Bartol and in Leeds. At Leeds a set of weights and curvature corrections was determined using system delays that were mea-

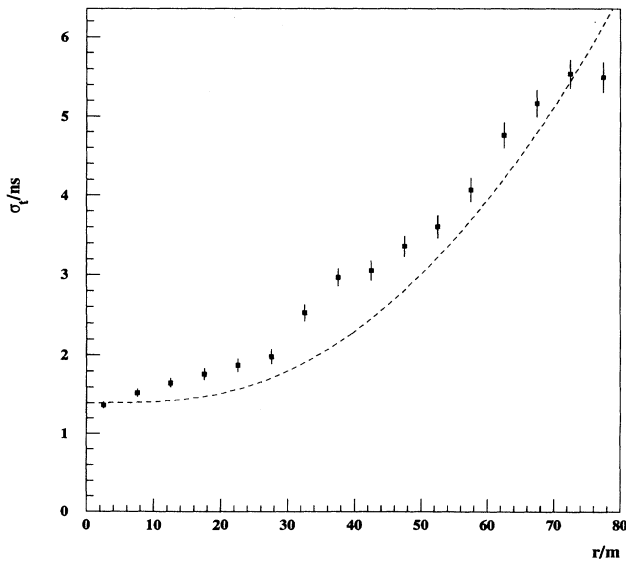


FIG. 9. The width of the timing residual distribution as a function of axial distance compared with the timing weight representation used in shower analysis.

sured before January 1992. At Bartol a parametrization was derived by using a more recent set of delays, measured in January 1992. The formulas are given by

$$dt_{\text{Leeds}}(r, S) = 0.04r + (5.44 + 0.0015r^2)/\sqrt{S}, \quad (4)$$

$$dt_{\text{Bartol}}(r, S) = 0.083r + 0.13r/\sqrt{S}, \quad (5)$$

$$\sigma_{\text{Leeds}}^2(r, S) = (0.1 + 0.1r)^2/S + 0.36, \quad (6)$$

$$\sigma_{\text{Bartol}}^2(r, S) = (1.5 + 0.047r)^2/S^{0.77}. \quad (7)$$

Here r is the distance in the shower plane to the core in meters, S is the recorded particle density per m^2 , dt is the time delay behind the shower plane in ns, and σ is the uncertainty associated with the recorded time, also in ns.

A spurious time recorded at any detector will have a great effect on the assigned arrival direction of the primary cosmic ray because of the small number of detectors in the array. A spurious time may arise from noise pulses in the recording system, from particles not associated with the shower front, or from the statistical response of the detectors to the particle front giving rise to a late signal. A spurious time will contribute greatly to the overall normalized τ^2 of the fit to the shower front timing data, and thus large τ^2 values may be used to identify deviant values and hence permit the rejection of the appropriate detector. In the analysis of the SPASE data, if the final normalized τ^2 of the shower front fit is greater than two, then the detector with the greatest contribution to the overall τ^2 is dropped from the fitting algorithm and the arrival direction is subsequently recalculated. This iterative procedure continues until the normalized τ^2 is below the preset limit or there are too few detectors remaining to allow the direction to be calculated. In the latter case the shower is discarded. Table III shows the frequency with which detectors are dropped in the arrival direction fitting procedure. By rejecting these spurious times it was possible to assign arrival directions to 98% of selected showers.

One special case exists for rejecting detectors from the arrival direction fitting algorithm. When large particle densities are recorded in certain detectors it is found that signal pick-up occurs in the discriminator rack which can cause other timing discriminators to trigger. This "cross talk" only occurs between certain detector pairs and after a well-defined delay of approximately 15 ns. The detector inducing the "cross talk" is referred to as the "master," those detectors that are spuriously triggered are termed the "slaves." Before the arrival direction is determined those detector pairs susceptible to cross talk are checked and any slave detector firing within a small window about

TABLE III. Frequency of dropping a detector in the arrival fitting procedure.

No. of detectors dropped	No. of events (%)
0	88.7
1	8.4
2	1.7
> 2	1.2

the well-defined delay are temporarily dropped from the fit. After the arrival direction has been calculated any slave detector dropped which recorded a time within 2 standard deviations of that expected is reinstated and the arrival direction redetermined. The number of showers in which cross talk is experienced is relatively small, some 0.8% of the data set.

The location of the core of the extensive air shower may be determined in several ways. A minimization of the quantity

$$\chi^2 = \sum_{\text{all dets}} \left(\frac{s(i)_{\text{obs}} - s(i)_{\text{expt}}}{\sigma(i)} \right)^2,$$

where $s(i)_{\text{obs}}$ and $s(i)_{\text{expt}}$ are the observed and predicted particle densities at each detector and $\sigma(i)$ is the associated uncertainty in the expected value, leads to a core, but is costly in terms of computational power. This is due to a large number of local minima and maxima in the χ^2 surface which arise as the lateral distribution function used to describe the particle densities expected across the shower front tends to a singularity at small axial distances, i.e., when the core is placed near a detector. From simulations the core determined by a minimization of χ^2 is found to have a rms shift of 7 m from the true core.

A center of gravity core may be quickly calculated with the best approximation to the true core being obtained when the detector coordinates are weighted according to the square of the observed particle density [6]. The rms shift between the center of gravity core and the true core has been determined for the SPASE array to be ~ 6 m, again from simulated showers. This is comparable to the error in χ^2 minimization core owing to the small separation between detectors and the small number of detectors within the array.

A major drawback of the center of gravity technique is that the core is always placed inside the array boundary. For a small array, such as SPASE, it is important to know whether the core of the shower has landed inside the perimeter of the array, since reconstruction of the arrival direction is only possible when the core position can be accurately estimated. Simulations have shown that approximately 50% of the air showers that trigger the SPASE array actually have cores falling outside the array boundary. Any selection criterion will result in the following subcategories: Accepted showers, rejected showers, falsely accepted showers, and falsely rejected showers. The ‘‘contamination’’ (C) and ‘‘loss’’ (L) percentages can be quantified as follows:

$$C = \frac{N_{\text{FA}}}{N_{\text{ac}} - N_{\text{FA}}} \times 100\%,$$

$$L = \frac{N_{\text{FR}}}{N_{\text{ac}} - N_{\text{FA}}} \times 100\%,$$

where N_{FA} is the number of falsely accepted showers, N_{FR} is the number of falsely rejected showers, and N_{ac} is the total number of accepted showers. The normalization is with respect to the number of showers that have been correctly accepted: $N_{\text{ac}} - N_{\text{FA}}$.

To determine whether the core actually fell outside the array boundary two techniques are applied. Prior

to the construction of the guard ring detectors any core landing beyond a 40 m radius of the array center, i.e., falling close to the array edge, is rejected. The contamination percentage for this simple distance cut is approximately 50%. Out of 1000 showers, approximately 250 are discarded, while 750 events survive the 40 m distance cut. However, 250 of these accepted events really have cores outside the array perimeter, leading to a value of $C = 250/(750 - 250) = 50\%$. A consideration of the areas involved leads to an estimate for the loss percentage of about 25%. After the construction of the guard ring the density information from these detectors may be used to assess core location. As an alternative to the distance cut, a neural network pattern recognition system has been developed [7] to detect and discard showers that landed outside the boundary. This results in a contamination of 9%, and a loss percentage of 13%. The majority of the incorrectly accepted and rejected events are located near the array boundary, which makes the contamination less of a concern, as the core of these events can still be located without problems.

Extensive air showers used in the search for ultrahigh energy γ -ray emission are selected from the recorded data if they satisfy the following criteria: (i) The core is located within the boundary of the main array consisting of the 16 timing detectors; (ii) at least five detectors have recorded particle densities greater than 1 m^{-2} ; (iii) there are at least four detectors with usable timing measurements of the shower front; (iv) the timing fit to the shower front has a normalized τ^2 below an arbitrarily set threshold of 10.

The number of events satisfying these criteria for each data epoch is given in Table II.

V. ANGULAR RESOLUTION AND POINTING ACCURACY

When using a telescope to search for γ -ray emission from an astrophysical object it is important to assess the angular resolution of the telescope so that an optimum search technique may be applied to resolve the small signal from the large background of cosmic ray showers. It is also important to know the uncertainty in the direction in which the telescope is pointing. For an extensive air shower array these parameters are not easily determined as there are no unambiguous astronomical sources which may be used as a ‘‘candle’’ and no terrestrial equivalent. The technique of searching for the shadow cast by the Moon and Sun in the cosmic ray background used at other extensive air shower sites [8] is not possible due to the high latitude of the South Pole.

The pointing accuracy of the SPASE telescope has been determined by operating the air shower array in coincidence with air Čerenkov detectors located nearby. An air Čerenkov telescope has a definite optical axis that may be measured directly and only extensive air showers that have an arrival direction close to the optical axis of the air Čerenkov telescope will trigger both detectors.

TABLE IV. Difference between measured air Čerenkov telescope axis and arrival direction of coincident SPASE events.

Telescope	Zenith angle	Azimuth angle
GASP-SPASE difference	$-0.14^\circ \pm 0.39^\circ$	$-0.16^\circ \pm 0.53^\circ$
PSPACE-SPASE difference	$-0.09^\circ \pm 0.21^\circ$	$0.44^\circ \pm 0.51^\circ$

Two air Čerenkov telescopes have been utilized this way, a small test device called the Prototype South Pole Air Čerenkov Experiment (PSPACE) [9] used to assess the potential of the South Pole as an air Čerenkov observation site in 1989 and 1990, and the Gammas at South Pole (GASP) telescope [10,11] during 1990. The results from the analysis have been presented in Walker *et al.* [12]. Using the larger data set from 1990 the results from an analysis similar to that outlined in Walker *et al.* [12] are presented in Table IV, which gives the difference between the directly measured direction of the air Čerenkov telescope optical axis and that determined from the analysis of the coincident SPASE data. Combining the 1990 results gives a pointing accuracy for the SPASE telescope of $0.2^\circ \pm 0.5^\circ$. The surveyed directions of the air Čerenkov telescope optical axes are, for GASP a zenith angle of $27.7^\circ \pm 0.2^\circ$ and azimuth of $-3.2^\circ \pm 0.5^\circ$, and for PSPACE a zenith of $32.7^\circ \pm 0.2^\circ$ and azimuth of $-1.3^\circ \pm 0.5^\circ$. It can be seen that the pointing error of the SPASE telescope is consistent with zero and within the surveying error in determining the air Čerenkov telescope optical axis.

A common technique used to determine the angular resolution of air shower arrays is to split the array into two independent, interlocking sets of detectors. The arrival direction for a shower is determined by both “subarrays” and an estimate of the angular resolution of the array made from the difference in deduced directions. The measured parameter is the angular separation on the celestial sphere of these two directions, the “space angle” Ψ . The accuracy with which an arrival direction may

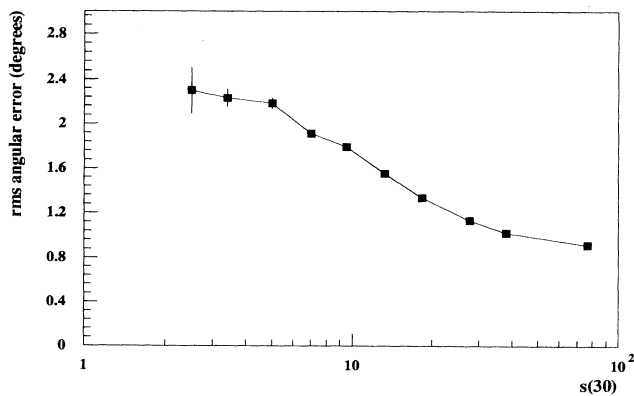


FIG. 10. The variation of the space angle between shower directions determined by subarrays as a function of shower size.

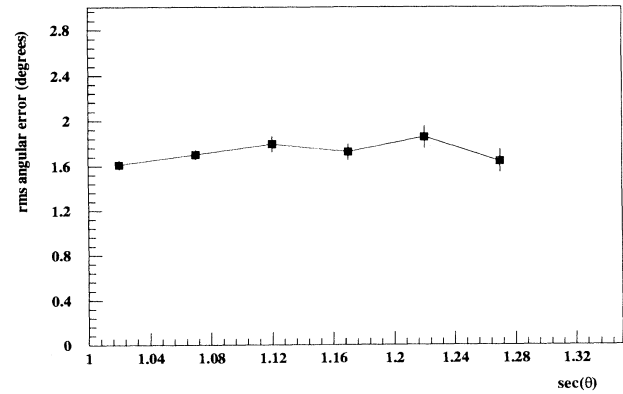


FIG. 11. The variation of the space angle between shower directions determined by subarrays as a function of the zenith angle of the shower.

be determined is dependent upon the zenith angle (or declination for the SPASE array) and size of the shower. Figures 10 and 11 show the variation of the space angle between the subarray directions as a function of shower size and declination, respectively. The shower size is measured in terms of the local ground parameter $s(30)$, the particle density recorded at a distance of 30 m from the shower axis. The relation between $s(30)$ and energy of the primary particle is shown on these figures for a shower arriving from the zenith. The angular resolution of an extensive air shower array is usually quoted as $\Psi/2$ to account for the increase in the number of detectors used in the fit and the directional uncertainty due to each subarray being equal. Weighting the variation in space angle according to the observed shower size spectrum gives an average angular resolution of 0.9° . When searching for emission from candidate sources these graphs may then be used to calculate the size of the optimum search area. Figure 12 shows the deduced optimum search box width

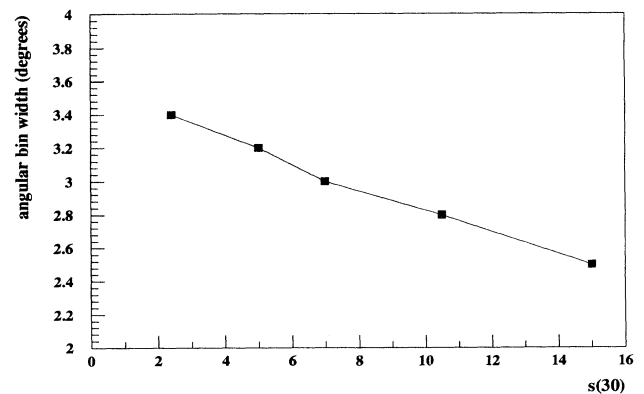


FIG. 12. The optimum search box width in declination for SN 1987A as a function of shower size.

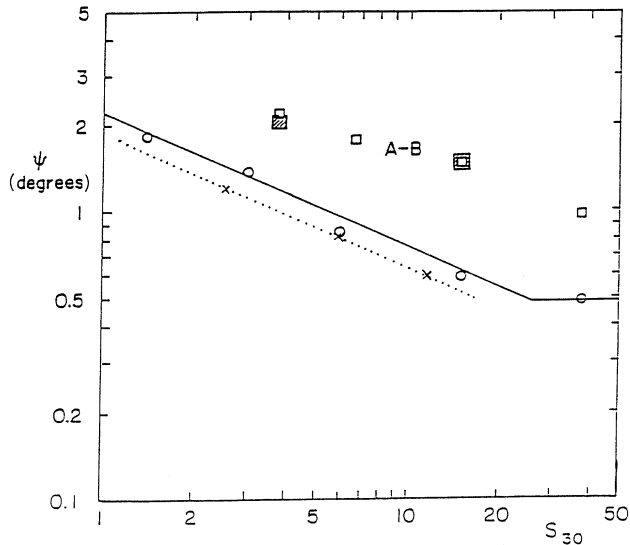


FIG. 13. The variation of angular resolution for γ -ray and proton-induced extensive air showers as a function of the density at 30 m from the shower core. Circles are for simulated proton showers and crosses for simulated photon showers. The lines indicate the trend of the data. The angular discrepancies between two subarrays (A and B) are given by the open squares for simulated showers and by shaded squares for observed showers.

in declination for SN 1987A as a function of shower size, incorporating the pointing uncertainty discussed above and a factor of 1.58 to maximize the signal-to-noise ratio. Weighting according to the observed shower size spectrum at that declination gives an average search box of 3.2° .

The subarray is an internal self-consistency check which is only applicable to the larger showers which trigger both subsets of detectors and is based upon the cosmic-ray-induced background showers rather than the γ -ray-induced showers of interest. However, from Monte Carlo simulations it is possible to assess whether γ -ray and cosmic-ray-induced showers may be equally well re-

constructed and to determine the angular resolution at lower energies. Smith *et al.* [1] show that the simulated showers yield similar results for both γ -ray and proton-induced showers, and that these results agree well with recorded data. Figure 13, reproduced from Smith *et al.* [1], shows the angular resolution for γ -ray and proton-induced showers as a function of primary energy for simulated and observed showers.

VI. CONCLUSIONS

It has been shown that the South Pole Air Shower Experiment has been operating in a stable condition since its inception in December 1987 to the austral summer of 1992. Typical variations in the timing delays for the scintillation detectors over this four year period are seen to be 200 ps, a value which is better than attained in similar experiments in more temperate regions. Two independent analysis programs have been developed which return nearly identical arrival directions for the primary cosmic ray which increases the confidence in these directions determined. The uncertainty in the arrival direction calculated for a shower has been shown to be 0.5° for the largest 5% of showers, increasing to 1.2° for the smallest 10% of events. The uncertainty in the pointing direction of the array has been evaluated from air Čerenkov telescopes to be less than 0.2° . The results of searches for ultrahigh energy γ -ray emission from point sources using the analyzed data from the SPASE telescope are given in a separate paper [3].

ACKNOWLEDGMENTS

We thank P. A. Ogden, M. Patel, G. Wright, A. Price, D. Pearce, L. Shulman, A. Walker, M. Finnemore, K. Chan, P. Surrey, S. Bloomer, and R. J. O. Reid for their contributions in the design and construction of the telescope and obtaining the observations. We thank J. Linsley for donating the scintillator. This work has been funded in part by NSF Grant No. DPP-9117524 and SERC Grant No. GRG 35923.

- [1] N. J. T. Smith *et al.*, Nucl. Instrum. Methods A **276**, 622 (1989).
- [2] A. M. Hillas, in *Proceedings of the 1986 Vulcano Workshop on High Energy-Ultrahigh Energy Behavior of Accreting X-ray Sources*, edited by F. Giovanelli and G. Mannocchi (Editrice Compositori, Bologna, 1986), p. 331.
- [3] J. van Stekelenborg *et al.*, following paper, Phys. Rev. D **48**, 4504 (1993).
- [4] S. D. Bloomer, J. Linsley, and A. A. Watson, J. Phys. G **14**, 645 (1988).
- [5] M. Finnemore *et al.*, in *Proceedings of the 22nd International Cosmic Ray Conference*, Dublin, Ireland, 1991,

- edited by M. Cawley *et al.* (Dublin Institute for Advanced Studies, Dublin, 1992), Vol. 1, p. 389.
- [6] D. W. Idenden, Ph.D. thesis, University of Leeds, 1992.
- [7] J. C. Perrett and J. T. P. M. van Stekelenborg, J. Phys. G **17**, 1291 (1991).
- [8] D. E. Alexandreas *et al.*, Nucl. Instrum. Methods A **311**, 350 (1991).
- [9] A. Walker *et al.*, in *Antarctic Journal of the United States*, edited by W. Reuning (NSF, Washington, D.C., 1990), Vol. 25-5, p. 273.
- [10] B. Morse *et al.*, in *Physics and Experimental Techniques of High Energy Neutrinos and VHE and UHE Gamma-Ray Particle Physics*, Proceedings of the Workshop, Lit-

- tle Rock, Arkansas, 1989, edited by G. B. Yodh, D. C. Wold, and W. R. Kropp [Nucl. Phys. B (Proc. Suppl.) **14A**, 61 (1990)].
- [11] J. Gaidos *et al.*, in *Physics and Experimental Techniques of High Energy Neutrinos and VHE and UHE Gamma-Ray Particle Physics* [10], p. 265.
- [12] A. Walker *et al.*, Nucl. Instrum. Methods A **301**, 574 (1991).